

Specific Detection of BTEX Contamination in Water

Using a π -Hole-Catching Surface Acoustic Wave

Sensor

Jean-Michel Friedt,^{[a]} Vincent Luzet,^[a] Valérie Soumann,^[a] Nathalie Nief,^[b] Bertrand Segues,^[b]
Gilles Pucheu,^[b] Jean-Sébastien Dehez,^[b] John-Richard Ordonez-Varela^[b] and Frédéric
Chérioux^{*[a]}*

^[a] Université de Franche-Comté, CNRS, FEMTO-ST, 15B avenue des Montboucons F-25000
Besançon, FRANCE

^[b] TotalEnergies OT/R&D-PERL, F-64170 Lacq, France.

ABSTRACT. Benzene, toluene, ethylbenzene, and xylene (BTEX) are volatile organic compounds that can contaminate groundwater resources, attracting significant attention due to their toxicity for human health and environment, and requiring the deployment of groundwater monitoring strategies. In this study, we demonstrate the selective detection of BTEX using a Surface Acoustic Wave (SAW) sensor coated with a polymer specifically designed to selectively interact with BTEX molecules. Since BTEX molecules can engage in π -hole interactions, we designed a polymer incorporating perfluorophenyl groups, to promote π -hole interactions. We then show that these π -hole interactions lead to excellent specificity of detecting BTEX contamination in water sources

over MTBE and ETBE interfering compounds. This novel approach holds promise for advancing the accurate identification of BTEX pollutants, addressing critical concerns in water quality assessment and management.

INTRODUCTION

Mono-aromatic hydrocarbons, specifically benzene, toluene, ethylbenzene, and xylenes (BTEX), are regulated as pollutants in groundwater and other water sources.¹ These contaminants often originate from the synthesis of other chemical compounds or release to the environment during their use as industrial solvents. Their presence in environment can result from industrial effluents, unintentional accidents or incidents such as oil spills, pipeline and storage leaks, or atmospheric pollution.^{2,3} Actually, the persistent presence of BTEX compounds in air has been reported, with these compounds being transported from the air to water bodies during rainfall.⁴ Ingestion of BTEX compounds has been associated with adverse health effects, including cancer, liver damage, drowsiness, and organ irritation. Prolonged exposure to BTEX compounds has been linked to skin and sensory irritation, respiratory problems, and central nervous system irritation⁵. BTEX are also recognized as highly toxic environmental compounds.

Most health or environmental protection agencies have established standards setting the highest level of a contaminant allowed in drinking water, known as the Maximum Contaminant Level (MCL), for BTEX. These values are approximately one part per million (ppm).⁶ Groundwater monitoring entails extracting water samples from wells situated upstream to the target location and analyzing them for potential pollutants. This procedure is efficient but also time-consuming, labor-intensive, and costly.^{7,8} In addition, the method of sampling and preserving BTEX molecules in

water is challenging due to their high volatility. A more efficient solution would be to deploy automated sensor systems within the wells, conducting periodic assessments of water quality. On the one hand, commercially available fluorometers⁹ or portable gas-chromatography coupled with mass spectrometers¹⁰ have been developed as sensitive physical tools for the detection of BTEX in groundwater. On the other hand, chemosensors based on electrical^{11,12} or optical properties have also been developed.^{13,14} Finally, quartz crystal microbalance (QCM)¹⁵ or surface acoustic waves (SAW), both coated with polymer,^{16,17,18,19} have also been used for the detection of BTEX in water, achieving detection limits for BTEX molecules at the parts per billion (ppb) level.¹⁹ However, in most cases, polymers used as a sensitive layer do not exhibit a tailored ability to recognize or interact specifically with BTEX molecules because they are only able to promote non-specific interactions with BTEX molecules. This lack of selectivity has been partially circumvented by using signal processing.^{17,20} To address the selectivity of sensors, we have developed an effective approach combining supramolecular chemistry. Furthermore, the resulting polymer was formulated to be compatible with uniform thin films spin coating on the surface of SAW sensors. This combination delves into the promotion of quadrupole-quadrupole interaction,²¹ a stronger noncovalent force between BTEX molecules and electron-deficient aromatic rings than the previously used π - π interactions for BTEX sensing.²² We demonstrate that this strong and specific quadrupole-quadrupole interaction, called π -Hole interaction, definitely promotes the selectivity of the detection of BTEX analytes in water at the ppm level. The detection of BTEX molecules is achieved by using a SAW sensor coated with a polymer designed for promoting π -Hole interaction.

EXPERIMENTAL SECTION

Synthesis of 2,3,4,5,6-pentafluorobenzylmethacrylate

7 mL of methacrylic anhydride (47 mmol) are added to 10 g of 2,3,4,5,6-pentafluorobenzyl alcohol (1.1 eq.) The mixture is heated up to 110°C for 4 hours. After cool down the methacrylic acid is extracted from the crude oil with a 10%(w/v) solution of potassium carbonate. The desired compound is then isolated by distillation under reduced pressure as a colorless oil (Boiling point 104°C at 28 mBar). Yield > 90%. NMR spectra are described in Figures S1-3 in SI.

Poly(2,3,4,5,6-pentafluorobenzylmethacrylate)

The previously synthesized monomer is degassed with nitrogen for 15 min. A catalytic amount of benzoyl peroxide is added and the reaction is heated to 100°C. The stir bar is blocked after few minutes by the solidification of the polymer but the temperature is kept still for 2 hours. The obtained translucent block is dissolved overnight in 15 mL of dichloromethane. The obtained solution is precipitated in 150 mL of methanol. The filtrated white powder is dissolved again to repeat the process twice. pPFBMA is obtained as a white powder. NMR spectra are depicted in Figures S4-5 in SI.

Size Exclusion Chromatography (SEC) analysis of polymers was carried out at 35°C using THF as eluent with a complete Shimadzu set-up (including LC-20AD, DGU-403, SIL-20A, CTO-20A and SPD-M20A). Typically, the polymer solution was prepared at 4 mg·mL⁻¹ and then filtered through 0.45 µm PTFE filter (Chromafil Xtra from Macherey-Nagel) to remove insoluble residues.

Differential scanning calorimetry (DSC) were achieved by using a DSC3 apparatus from Mettler Toledo by using Aluminum-crucibles (40mL) under a flux of nitrogen (50 mL·min⁻¹) with a temperature speed of 20°C·min⁻¹.

Fabrication of functionalized SAW sensors

The sensor is manufactured on a 36°-rotated, Y-cut, X-propagating lithium tantalate (LiTaO₃) piezoelectric substrate (LT), recognized for its effective performance in liquid settings. The SAW device is designed as a reflective-delay-line with differential measurements to reduce the influence of temperature on readings. The aluminum interdigital transducers (IDTs) patterned on the piezoelectric substrate have a periodicity of 40 μm, leading to a working frequency f centered on 100 MHz. The echo magnitude provides a coarse delay estimate, but the fine acoustic velocity (v) measurement is deduced from the phase measurement (φ) since a mirror patterned at distance D from the interdigitated transducer induces a time delay $\tau=D/v$ leading to $\varphi=2\times\pi\times f\times\tau$. In our case, the distance D to the mirror reflecting the strongest signal is equal to 4700 μm.

Reflective delay lines are characterized in the time domain but measured in the frequency domain using a vector network analyzer and computing digitally the inverse Fourier transform. Figure S6 displays the reflection scattering coefficient S_{11} interpreted as a broad transfer function from 95 to 105 MHz attributed to the interdigitated transducers (IDTs) and a sharp interference pattern resulting from the sum of the echoes reflected by the mirrors back to the IDT. The interference pattern of the multiple echoes reaches nearly -10 dB, hinting at a good impedance matching and energy transfer from electrical to acoustic wave. The number of probed frequencies is selected by considering the longest echo delay: when characterizing in the spectral domain over a bandwidth B sampled with N equally spaced frequencies, then the maximum delay after inverse Fourier transform is N/B . Here with $B=40$ MHz, a maximum echo delay of 5 μs requires sampling $N=200$ discrete frequency steps. Computing the inverse Fourier transform of this spectral domain characterization leads to Figure S7 where the first echo insertion losses are in the -40 dB range.

Notice though that the frequency domain to time domain inverse Fourier transform spreads energy in different parts of the chart and the insertion loss value might not be related to the classical S_{21} value in the -15 to -20 dB range for lithium tantalate transmission line devices. Nevertheless, as shown on Figure S7, the signal to noise ratio is excellent with a baseline around -70 dB, allowing for an accurate measurement of the phase of the third echo (Figure S7, bottom, dashed vertical line) referenced to the first echo.

To achieve the functionalization of LT substrate, LT surface as well as aluminum IDTs were previously functionalized by Ti Prime, an adhesion promoter improving resist adhesion on oxide-type substrates. Then, a drop of a 1,2-dichloroethane solution containing pPFBMA at a concentration of $150 \text{ g}\cdot\text{L}^{-1}$ was spin-coated (acceleration, 900 rpm/s; speed, 3000 rpm; duration, 30 s) onto a diced chip including four SAW reflective delay lines in parallel for reproducibility assessment. Finally, the film is annealed at $120 \text{ }^\circ\text{C}$ for 120 min. This procedure leads to the formation of a solid thin film (thickness, $700 \pm 100 \text{ nm}$; measured by mechanical profiler) which covers entirely the sensing area and IDTs. The same procedure was applied for the deposition of polystyrene used for the control experiment (purchased from Sigma-Aldrich, $M_w = 280,000 \text{ g}\cdot\text{mol}^{-1}$), resulting in a layer with a thickness of $330 \pm 50 \text{ nm}$.

Calibration of BTEX-water mixture

The concentration of BTEX (Benzene, Ethylbenzene, Toluene, Xylene) in water solutions was measured using UV-visible spectroscopy, with a Perkin Elmer Lambda 365 instrument. To do this, we first determined the molar absorption coefficient for each BTEX molecule in water. These coefficients are as follows: Benzene absorbs at 254 nm with a coefficient of $1491 \text{ L}\cdot\text{mol}^{-1}\cdot\text{cm}^{-1}$, Toluene at 261 nm with a coefficient of $300 \text{ L}\cdot\text{mol}^{-1}\cdot\text{cm}^{-1}$, Ethylbenzene at 261 nm with a coefficient of $223 \text{ L}\cdot\text{mol}^{-1}\cdot\text{cm}^{-1}$, and Xylene at 261 nm with a coefficient of $335 \text{ L}\cdot\text{mol}^{-1}\cdot\text{cm}^{-1}$.

Then, the concentration of BTEX in the water samples used for exposing the BTEX sensor was determined. This was achieved by sampling the mixture and analyzing it using UV-visible spectroscopy.

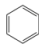
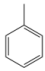
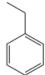
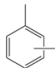
RESULTS

BTEX molecules belong to the family of volatile organic compounds, characterized by their construction around a monocyclic aromatic hydrocarbon ring comprised of six carbon atoms (refer to Table 1). Due to the aromaticity of their core skeleton, BTEX molecules exhibit low reactivity. Primarily, they undergo electrophilic aromatic substitution reactions, necessitating Lewis acids (such as AlCl_3) or strong Brønsted acids (like sulfuric acid) as catalysts.²³ This low chemical reactivity makes BTEX molecules useful solvents in various reactions. However, this also makes them resistant to most degradation processes by living organisms and environmental factors, leading to their long-term persistence and consequent high toxicity.

Due to the limited chemical reactivity of BTEX molecules, developing sensitive layers with high selectivity for these compounds is still challenging. Nonetheless, the central monocyclic aromatic hydrocarbon ring of BTEX imparts specific physicochemical properties to these molecules. It is notable that BTEX molecules exhibit a dual nature, acting as persistent pollutants in soils due to their hydrophobicity (as indicated by their low organic carbon-water partition coefficient, K_{oc} , see Table 1), while also being soluble in water (evidenced by their low *n*-Octanol/Water Partition Coefficient, Log P, see Table 1). This intriguing duality is fully elucidated by the structure of BTEX molecules.

The higher electronegativity of carbon compared to peripheral hydrogen atoms results in an accumulation of electron density in the delocalized π -bonds within the carbon skeleton of BTEX

molecules (see Table 1). Consequently, these molecules possess a negatively charged quadrupole moment, facilitating strong interactions with water molecules, which are dipolar, thereby enhancing their solubility in water.²⁴ However, despite the importance of electrostatic interactions, existing BTEX sensors have predominantly relied on dispersion forces, sacrificing selectivity. We propose leveraging the specific charge distribution of BTEX molecules to design a sensitive and selective polymer. Given that electrostatic interactions depend closely on the charge distribution within the involved molecules, a precise understanding of molecular charge distribution is essential for harnessing these interactions effectively. Given the electron-rich nature of the aromatic core in BTEX molecules, they have the capability to engage in electrostatic interactions with molecules possessing an electron-deficient aromatic ring. This interaction can be achieved by replacing peripheral hydrogens with more electronegative elements such as fluorine, which alters the electron distribution within the π -bond system, resulting in an electron-deficient state and consequently generating a positive quadrupole moment for the molecule. This process creates a π -electron-deficient void in the central region of the molecule, commonly referred to as a π -Hole.^{25,26,27}

	Benzene	Toluene	Ethylbenzene	Xylenes
Formula	C ₆ H ₆	C ₇ H ₈	C ₈ H ₁₀	C ₈ H ₁₀
Structure				
Molecular weight (g/mol)	78.12	92.15	106.18	106.18
Density	0.8765	0.8669	0.8670	0.8685

Solubility in water (g/L)	1.70	0.50	0.15	0.15
Soil-water partitioning coefficient (log K_{oc})	1.99	2.38	2.79	2.76
Octanol-water partitioning coefficient (log P)	2.03	2.52	3.17	3.15
Toxicity	Carcinogen: group 1	Carcinogen: group 1	Carcinogen: group 1	Carcinogen: group 1

Table 1. Physical and chemical properties and toxicity of BTEX molecules. K_{oc} measures the mobility of a substance in soil (low K_{oc} = strong mobility). K_{oc} is a very important input parameter for estimating environmental distribution of a chemical substance. P (also named K_{ow}) measures the ratio of the concentration of a chemical in *n*-octanol and water at equilibrium at a specified temperature. Low log P (below 4.5) indicates a good affinity for water.

With the above concerns as context, we have designed a polymer, the 2,3,4,5,6-pentafluorobenzylmethacrylate (pPFBMA), that can be used as highly-selective layer towards BTEX on a direct detection sensor including SAW by using π -hole interaction. Our molecular design is based on a perfluorophenyl group, acting as the π -hole site (highlighted in red, Figure 1a) and a methacrylate group, which can be easily polymerized (in blue, Figure 1a).

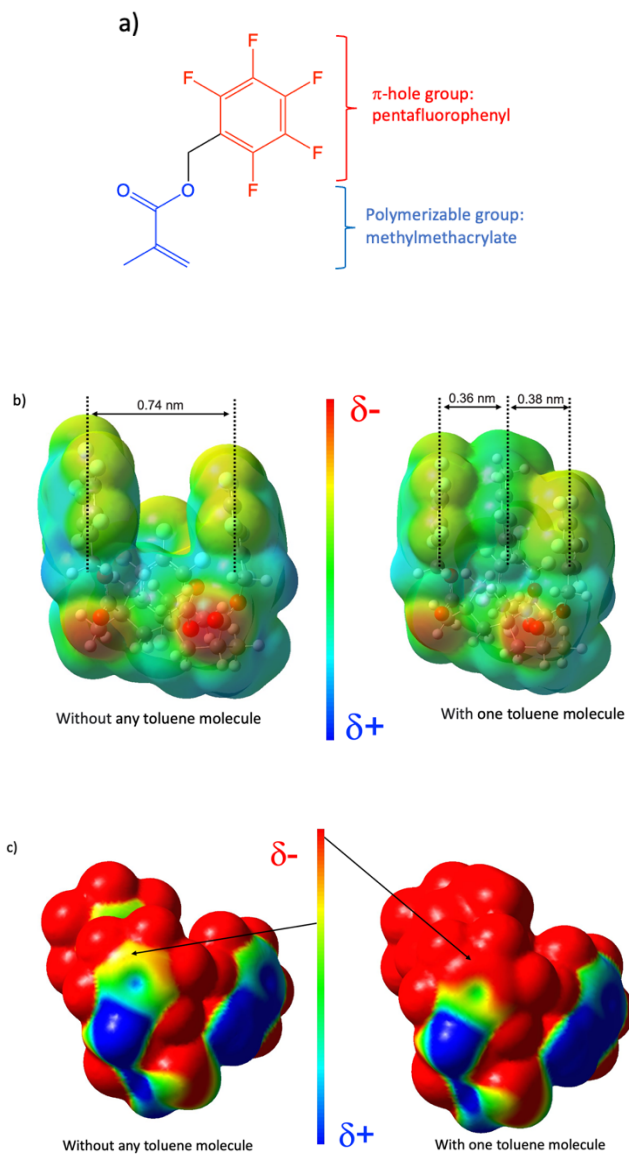


Figure 1. Scheme caption. a) Molecular design for the BTEX detection. b) CPK model of a trimer of pPFBMA including no (left) or one toluene molecule (right) and corresponding electrostatic potential map, coloured surface from positive (blue) to negative charge (red). c) The color scale has been chosen to highlight the increase of the electrostatic potential map of perfluorophenyl groups of the polymers due to the presence of one toluene molecule, as highlighted by the two arrows.

To assess whether the molecular design we conceived can effectively detect BTEX molecules through π -hole interaction, we optimized the geometry of a trimer of pPFBMA using Gaussian 09 software at the B3LYP/6-311G(d,p) density functional level.²⁸ The optimized geometry shows a cavity formed by two pentafluorophenyl groups, resulting from the displacement of the pentafluorophenyl ring that was initially situated between the other two rings. The distance between two pentafluorophenyl moieties surrounded the cavity remains at 0.74 nm (see Figure 1b and video in SI). Then, the geometry of a trimer of pPFBMA including a molecule of toluene in the cavity was optimized. Upon calculation, the distances between the pentafluorophenyl moieties and the toluene molecule were found to be 0.36 and 0.38 nm, respectively, whereas initially, the toluene molecule was placed near one of the two pentafluorophenyl moieties (see Figure 1b). These distances are longer than those calculated in the case of a $C_6H_6 \cdots C_6F_6$ dimer (0.33 nm).²⁷ However, toluene is found at an equidistance between two pentafluorophenyl moieties to interact with both of them. Regarding the total interaction energy, defined as the difference in total energy between the trimer with a toluene molecule and the trimer without a toluene molecule, the presence of the toluene molecule leads to a stabilization of $4.46 \text{ kJ}\cdot\text{mol}^{-1}$. This energy is slightly lower than that calculated in the case of a $C_6H_6 \cdots C_6F_6$ dimer ($6.3 \text{ kJ}\cdot\text{mol}^{-1}$)²⁷, which aligns with the longer distance between toluene and pentafluorophenyl moieties compared to the $C_6H_6 \cdots C_6F_6$ dimer. The five other molecules of the BTEX family can fit into the cavity formed by two pentafluorophenyl moieties (see Figure S8 in SI).

To emphasize the role of π -Hole interaction, we depicted the electrostatic potential map of a trimer with and without a toluene molecule (see Figure 1c and Figure S9 in SI). The color scale for both images was chosen to highlight the pentafluorophenyl ring surrounding the toluene molecule (Figure 1c, right). It is observed that the pentafluorophenyl rings of the trimer

surrounding a toluene molecule are more electron-rich than those without any toluene molecule in the cavity. In addition, there is also a charge transfer from the nodal plane of pPFBMA trimer (including fluorine atoms) to the nodal plane of the toluene molecule included in the cavity (See Figure S9 in SI). This reorganization of the electron density of pPFBMA trimer and toluene molecules results from the π -hole interaction between them. To confirm this result, we also performed DFT simulations on a trimer in which the three pentafluorophenyl rings were replaced by phenyl rings. In this case, the toluene molecule does not remain within the cavity as observed in the pPFBMA trimer. Instead, it is ejected from the cavity and adopts a parallel-displaced geometry²⁷ to optimize electrostatic interactions between the toluene molecule and the phenyl rings (see Figure S10 in SI). Finally, DFT simulations indicate the existence of a cavity formed between the pentafluorophenyl groups within pPFBMA. This cavity possesses dimensions and electronic characteristics that are suitable for selectively capturing BTEX molecules by π -hole interactions.

pPFBMA was synthesized in two steps (Figure 2). 2,3,4,5,6-pentafluorobenzylmethacrylate (PFBMA) molecule was prepared in high yields from methacrylic anhydride and 2,3,4,5,6-pentafluorobenzyl alcohol (see method section and Figures S1-3 in SI). Then, pPFBMA was synthesized by radical polymerization without any solvent.²⁹ pPFBMA was then isolated by precipitation into methanol (See method section and Figures S4-5 in SI).

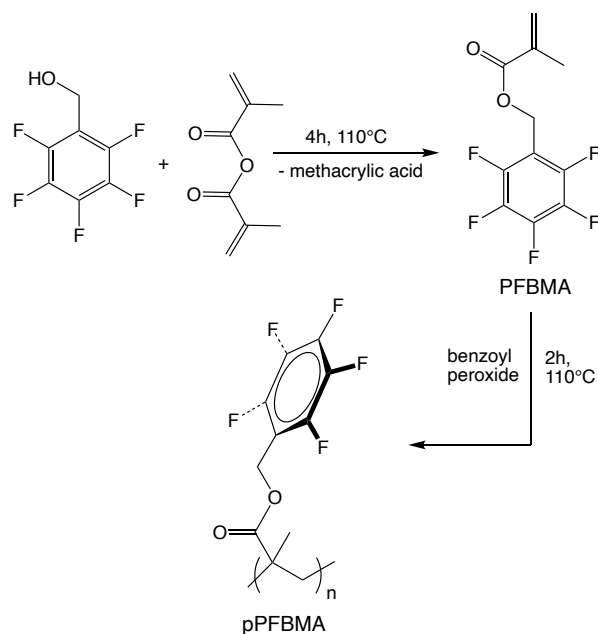


Figure 2. Scheme of synthesis of the designed polymer pPFBMA.

The weight-average molecular weight (M_w), number-average molecular weight (M_n), and dispersity (M_w/M_n) of pPFBMA were determined using Size Exclusion Chromatography (SEC) analysis. For a typical polymerization time of 4 hours, M_w equals $117,800 \pm 1,000 \text{ g} \cdot \text{mol}^{-1}$. The corresponding M_n is $30,000 \pm 5,000 \text{ g} \cdot \text{mol}^{-1}$, resulting in a dispersity of 4.4 ± 1 . This dispersity is larger than expected for a radical polymerization, which can be attributed to the absence of a solvent that would limit monomer diffusion at the end of the polymerization process.³⁰

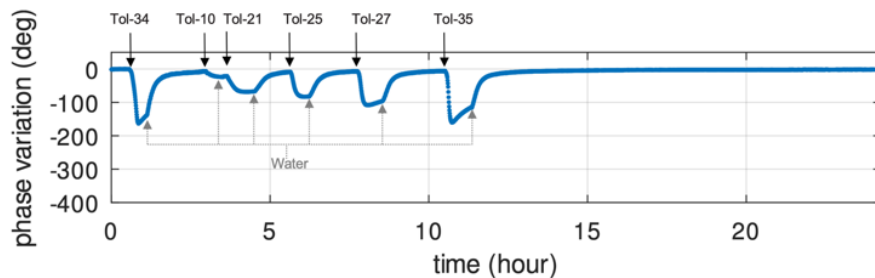
The glass transition temperatures (T_g) were also determined using differential scanning calorimetry (DSC). The experimental value of T_g is $77.5 \pm 0.5^\circ\text{C}$, falling within the range of values measured for other fluorinated polymers.³¹ The low T_g of pPFBMA is due to the presence of fluorine atoms. A polymer with low T_g is a much better candidate for sensing applications because the absorption/diffusion/desorption of analytes is promoted by the mobility of polymer chains.¹⁹

Sensing of BTEX in water solution by using a SAW sensor

A SAW sensor is based on SAW electrodes, which are patterned onto a lithium tantalate (LT) substrate, acting as a reflective delay line with four Bragg mirrors introducing delays varying with the acoustic velocity tuned by mass loading (density) and polymer stiffness.³² The sensitive layer is made of a thin film (thickness: 700 ± 100 nm) of pPFBMA deposited by spin coating onto the LT substrate (see details in Method section). The operating frequency of the SAW sensor is 100 MHz. Since pPFBMA is spin coated and globally covers the whole SAW sensor, we have opted for echo number 3, as it offers the optimal balance between maximizing delay and signal level (See Figures S6-7). Hence, in all further charts, the phase evolution from its baseline is displayed as a function of time as experiments are being conducted of exposing the SAW sensor to various solutions. In a first experiment, we aim at demonstrating the capability of a thin solid film of pPFBMA to detect efficiently BTEX molecules in a water solution. A typical experiment is based on the immersion of a functionalized SAW sensor in a water solution including a chosen BTEX molecule. The complex (real and imaginary part) transfer function of the SAW delay line is recorded by an Agilent technologies E5071B Vector Network Analyzer (VNA) in the 100 ± 10 MHz range (See Figures S11-12 in SI) leading to a phase measurement with a noise (one standard deviation) of 0.3° with a 30 second sweep duration (measurement refresh rate). The first experiment was made by exposure of the SAW device to water containing toluene (34 ppm), leading to a strong decrease of the phase (-165° , Figure 3). After 45 min of exposure, the decrease of the phase is stopped as the asymptotic limit is reached and then the SAW device is rinsed with pure water (Figure 3) until the phase reached again the starting baseline. Then, five other cycles of exposure to water solution including toluene molecules and rinsing with pure water have been performed. For each concentration of toluene (varying from 10 to 35 ppm), a phase decrease is observed (varying from -67 to -165°), depending with the concentration of toluene. After each

rinsing, the starting baseline is reached again. The duration of the last rinsing step is 14h, in order to investigate the stability of the thin solid film of pPFBMA grafted onto the surface of the SAW sensor. To strengthen our hypothesis regarding the significant role of electrostatic interactions, enhanced by the presence of a perfluorophenyl ring, we coated an acoustic sensor with a polystyrene layer and exposed it to an aqueous solution containing 46 ppm of toluene (see Figure 13 in the SI). This exposure led to a minor phase shift of 3° , which can be attributed to nonspecific adsorption and represents less than 1% of the phase variation observed with the pPFBMA polymer. The baseline was fully restored after rinsing the sensor with pure water.

a)



b)

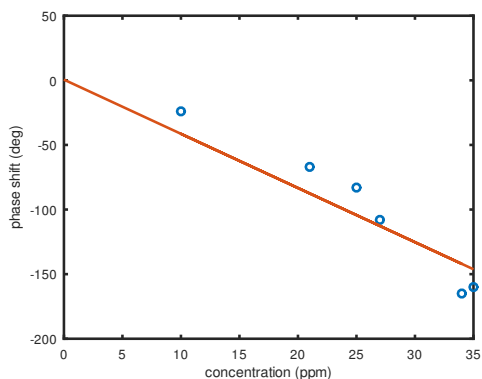


Figure 3. a) Detection of toluene in water solution. Evolution of the phase as a function of time of a SAW sensor, functionalized by a layer of pPFBMA, exposed to water containing different concentrations of toluene. Each concentration is indicated in ppm. All exposures are followed by a rinsing with pure water solution. b) Evolution of the phase as a function of toluene concentration. The slope of the red line is -4.2 ± 0.1 ($^{\circ}$ /ppm), as determined by linear regression.

The capability of pPFBMA polymer to detect the four other molecules constituting the BTEX compounds is then investigated. As in the case of toluene, each molecule has been diluted into water and the concentration is determined by UV-visible spectroscopy. The SAW sensor is sequentially exposed to benzene, toluene, ethylbenzene and xylene with a rinsing step with pure water between each exposure to assess that the signal returns to baseline. The corresponding results are depicted in Figure 4.

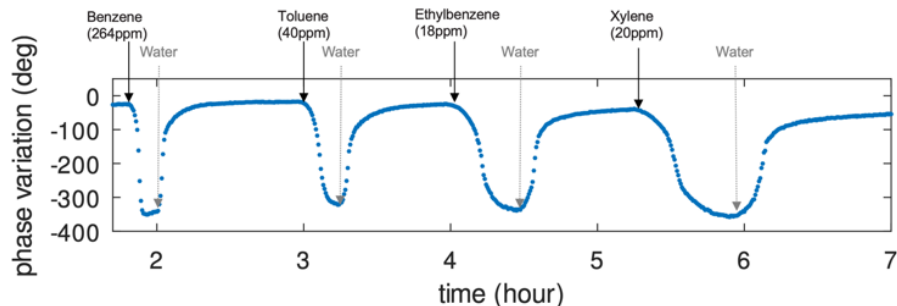
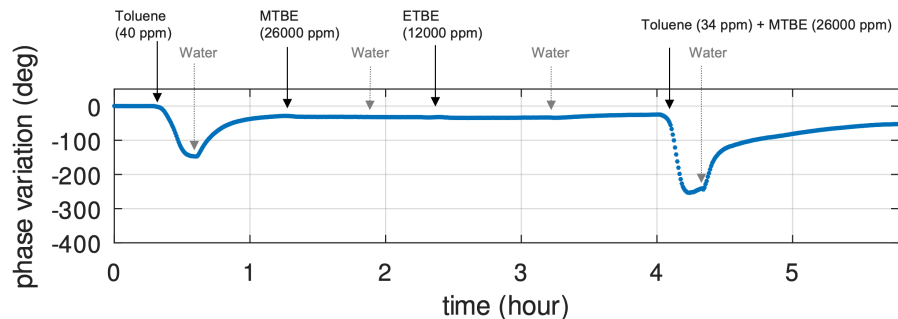


Figure 4. Detection of BTEX in water solution. Evolution of the phase as a function of time of a SAW sensor, functionalized by a layer of pPFBMA, exposed to water containing different concentrations of isolated BTEX molecules. Each exposure is followed by a rinsing with pure water solution.

Finally, the selectivity of pPFBMA polymer has been investigated. The main interferents which are commonly found in groundwater with BTEX molecules are methyl tert-butyl ether (MTBE), ethyl tert-butyl ether (ETBE) and cyclohexane because they have been added to gasoline to replace tetra alkyl-lead before 2000's.³³ Therefore, the effects of these interferents have to be managed because they are expected to interact with typical sensitive coatings used in BTEX sensors. After an exposition of the SAW sensor to a water solution containing 40 ppm of toluene (phase variation of -148°) followed by a rinsing with pure water, the SAW sensor was then exposed to a water solution containing 26,000 ppm of MTBE. No phase variation was observed (Figure 5). The SAW sensor was then exposed to 12,000 ppm of ETBE, and again, no detectable phase variation was observed. Finally, the SAW sensor is exposed to a mixture of MTBE (26,000 ppm) and toluene (34 ppm). The phase variation is -254° . The sensor is then rinsed with pure water during 1.5h (Figure 5). The same procedure was applied using cyclohexane (250 ppm) as an interferent. As with MTBE and ETBE, no phase shift was observed (see Figure S14 in SI). The sensor's ability to

detect toluene in water is not affected by exposure to these three interferents, as demonstrated by the final exposure to water-toluene solution (see Figures 5 and S14).

a)



b)

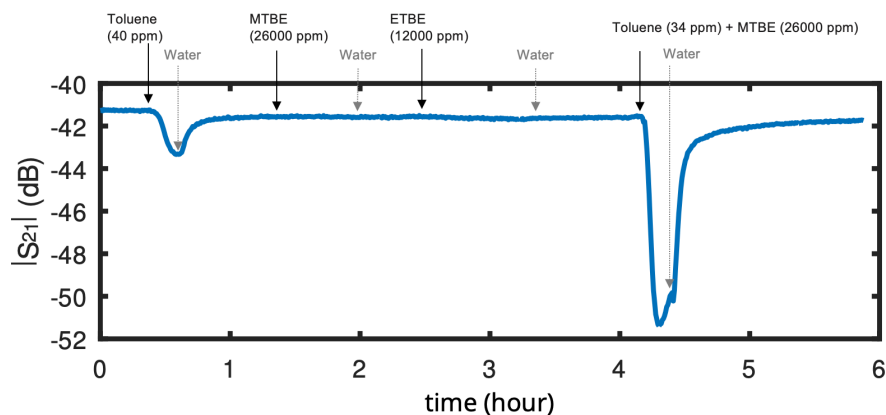


Figure 5. Specific detection of toluene in water solution. a) Evolution of the phase as a function of time of a SAW sensor, functionalized by a layer of pPFBMA, exposed to water containing toluene and then MTBE or ETBE as interferent. Each exposure is followed by a rinsing with a pure water solution. b) Insertion losses corresponding to the complete sequence described in a).

Regarding insertion losses, when the SAW sensor coated with pPFBMA is exposed to 40 ppm of toluene in water, the insertion losses rise by 2.3 dB. No insertion losses occur when the SAW sensor is exposed to MTBE or ETBE in water. However, when exposed to a mixture of toluene (40 ppm) and MTBE (26,000 ppm) in water, the insertion losses raise by 10.2 dB (Figure 5b). A final experiment was conducted to investigate the effect of exposing the sensor, functionalized with the pPFBMA polymer, to chlorinated solvents such as chloroform (8,000 ppm) and tetrachloromethane (1,000 ppm). Chloroform is an excellent solvent for this polymer while pPFBMA polymer is poorly soluble in tetrachloromethane. Following the same experimental protocol used for standard interferents, it was observed that exposure of the sensor to an aqueous solution saturated with either chloroform or tetrachloromethane resulted in a significant shift in the phase of the acoustic signal (see Figure S15 in SI).

DISCUSSION

The experimental results highlight the efficiency of π -Hole interaction for the BTEX sensing. Indeed, when the sensor coated with the polymer pPFBMA encounters varying levels of BTEX ranging from 10 to 264 ppm, it shows significant changes in phase decrease (-67° to -350° , Figure 4). In the absence of a perfluorophenyl ring, as observed when functionalizing SAW sensors with a polystyrene layer, exposure to an aqueous solution containing 46 ppm of toluene results in only negligible phase shifts (approximately 3°). In addition, our system measurement noise stands at around 0.3° , which is much lower than the fluctuations observed when exposed to different BTEX substances. To determine the detection threshold for toluene using this pPFBMA-coated SAW sensor, we consider the slope of the phase variation line relative to toluene concentration, which is approximately -4.2 ± 0.1 ($^\circ/\text{ppm}$). This yields a detection threshold of around 0.1 ppm. This

value aligns very well with the threshold of one part per million (ppm) required by environmental agencies worldwide.⁶ Measurements remain plagued by environmental fluctuations, most significantly temperature, when the polymer coated areas exhibit different temperature sensitivities than the uncoated areas used for reference, as well as hydrostatic pressure. Additionally, the reversible nature of BTEX capture by pPFBMA is evident from the phase returning to its initial state after rinsing with pure water. The very good sensitivity and the complete reversibility of the BTEX sensing observed with the SAW sensor functionalized by pPFBMA is based on the π -Hole interaction. While BTEX molecules are somewhat soluble in water, the perfluorophenyl ring's presence of pPFBMA results in significantly stronger electrostatic interactions with the electron-rich aromatic rings of BTEX than with water molecules. The sensor response times and phase variations increase with the size of the BTEX molecules (Figure 4), closely align with those observed in a SAW sensor functionalized with a polystyrene-plasticizer pair.¹⁹ All experimental data and numerical simulations strongly support the hypothesis that the diffusion of BTEX compounds into the pPFBMA polymer is enhanced, even in its glassy state, due to the stronger electrostatic interactions facilitated by the perfluorophenyl rings of the pPFBMA polymer.

In terms of selectivity, the SAW sensor remains unresponsive to MTBE, ETBE and cyclohexane interferents, even at high concentrations of up to 26% by mole, due to their aliphatic nature, coupled with their high miscibility in water. However, their presence enhances the sensor acoustic response to toluene. Notably, the phase decrease doubles when the sensor is exposed to a toluene+MTBE mixture compared to toluene alone (Figure 5a). However, the presence of these interfering molecules enhances the response of the SAW sensor when simultaneously exposed to BTEX. As demonstrated, upon exposure of pPFBMA thin solid film to a water-toluene mixture, toluene diffuses within the polymer layer, causing a change in its viscoelastic properties, as

indicated by the insertion losses of 2.3 dB (Figure 5b). This alteration also facilitates the diffusion of MTBE molecules into the polymer layer, further intensifying the changes in its viscoelastic properties as highlighted by the increase in insertion loss variations from 2.3 dB to 10 dB (Figure 5b). However, the diffusion of MTBE also increases the mass loading, resulting in a doubling of the phase decrease as well. A similar approach was made by adding plasticizer in polymer to increase their sensitivity thanks to the tuning of the viscoelastic properties.¹⁹ Consequently, the presence of interferents such as MTBE or ETBE enhances the sensor sensitivity to BTEX while maintaining its selectivity. The presence of chlorinated solvents, such as chloroform or tetrachloromethane, also alters the viscoelastic properties of the polymer layer, leading to a phase shift in the sensor signal. While this phenomenon might initially appear as a lack of selectivity of the sensor toward chlorinated solvents, it is important to highlight that their presence in groundwater represents a significant environmental pollution hazard.

CONCLUSION

In summary, this study demonstrates that π -Hole interactions serve as an effective method for detecting BTEX molecules in water by using acoustics sensors. π -Hole interactions leverage unique properties to enable sensitive detection that meets the standards set by global environmental agencies. Additionally, the method is highly selective, capitalizing on the inherent characteristics of BTEX molecules. This innovative approach paves the way for precise and sensitive detection of BTEX in water.

ASSOCIATED CONTENT

Supporting Information. All NMR spectra are fully described in the SI section (pdf file). The additional experimental data concerning the exposition to interferent are described. The cavity in the PFBMA trimer is highlighted in two video files (avi files).

The Supporting Information is available free of charge on the ACS Publications website.

AUTHOR INFORMATION

Corresponding Author

* jm.friedt@femto-st.fr and frederic.cherieux@femto-st.fr

Author Contributions

The manuscript was written through contributions of all authors. All authors have given approval to the final version of the manuscript. All authors contributed equally.

Funding Sources

This work is supported by the French National Agency through the project UNDERGROUND (ANR-17-CE24-0037). We also acknowledge partial support of the French RENATECH network and its FEMTO-ST technological facility.

ACKNOWLEDGMENT

We thank Dr. S. Benchabane (FEMTO-ST) for fruitful discussions.

REFERENCES

- (1) Yu, B.; Yuan, Z.; Yu, Z.; Xue-Song, F. BTEX in the environment: An update on sources, fate, distribution, pretreatment, analysis, and removal techniques. *Chem. Eng. J.* **2022**, *435*, 134825, DOI: 10.1016/j.cej.2022.134825

- (2) Fayemiwo, O. M.; Daramola, M. O.; Moothi, K. BTEX compounds in water – future trends and directions for water treatment. *Water SA* **2017**, *43*, 602-613, DOI: 10.4314/wsa.v43i4.08
- (3) Dehghani, M.; Abbasi, A.; Taherzadeh, Z.; Dehghani, S. E Exposure assessment of wastewater treatment plant employees to BTEX: a biological monitoring approach. *Sci. Rep.* **2022**, *12*, 21433, DOI: 10.1038/s41598-022-25876-x
- (4) Sostaric, A.; Stanisic Stojic, S.; Vukovic, G.; Mijic, Z.; Stojic, A.; Grzetic, I. Rainwater capacities for BTEX scavenging from ambient air. *Atmos. Env.* **2017**, *168*, 46-, DOI: 10.1016/j.atmosenv.2017.08.045
- (5) Davidson, C. J.; Hannigan, J. H.; Bowen, S. E. Effects of inhaled combined benzene, toluene, ethylbenzene, and xylenes (BTEX): Toward an environmental exposure model. *Environ. Toxicol. Pharmacol.* **2021**, *81*, 103518, DOI: 10.1016/j.etap.2020.103518
- (6) (a) U.S. Environmental Protection Agency can be found under <https://www.epa.gov/ground-water-and-drinking-water/national-primary-drinking-water-regulations>; (b) Environmental affairs can be found under <https://sawic.environment.gov.za/documents/562.pdf>; (c) Legifrance can be found under <https://www.legifrance.gouv.fr/loda/id/JORFTEXT000000465574>
- (7) Song, N.; Tian, Y.; Luo, Z.; Dai, J.; Liu, Y; Duan Y. Advances in pretreatment and analysis methods of aromatic hydrocarbons in soil. *RSC Adv.* **2022**, *12*, 6099-6113, DOI: 10.1039/D1RA08633B.
- (8) Khizar, S.; Zine, N.; Jaffrezic-Renault, N.; Elaissari, A.; Errachid, A. Prospective analytical role of sensors for environmental screening and monitoring. *Trends Analyt. Chem.* **2022**, *157*, 116751, DOI: 10.1016/j.trac.2022.116751.

- (9) Torion T-9 can be found under https://resources.perkinelmer.com/lab-solutions/resources/docs/gde_torion_t-9_gcms_users_guide.pdf.
- (10) Uvilux BTEX can be found under <https://chelsea.co.uk/products/uvilux-btex>.
- (11) Cooper, J. S.; Kiiveri, H.; Hubble, L. J.; Chow, E.; Webster, M. S.; Muller, K.-H.; Sosa-Pintos, A.; Bendavid, A.; Raguse, B.; Wiczorek, L. Quantifying BTEX in aqueous solutions with potentially interfering hydrocarbons using a partially selective sensor array. *Analyst* **2015**, *140*, 3233-3238, DOI: 10.1039/C5AN00223K
- (12) Ho, C. K.; Hughes, R. C. In-Situ Chemiresistor Sensor Package for Real-Time Detection of Volatile Organic Compounds in Soil and Groundwater. *Sensors* **2022**, *2*, 23, DOI: 10.3390/s20100023.
- (13) Myers, M.; Podolska, A.; Heath, C.; Baker, M. V.; Pejcic B. Pore size dynamics in interpenetrated metal organic frameworks for selective sensing of aromatic compounds. *Anal. Chim. Acta* **2014**, *819*, 78-81, DOI: 10.1016/j.aca.2014.02.004
- (14) Silva, L. I. B.; Panteleitchouk, A. V.; Freitas, A. C.; Rocha-Santos, T. A. P.; Duarte, A. C. Microscale optical fibre sensor for BTEX monitoring in landfill leachate. *Anal. Methods* **2009**, *1*, 100-107, DOI: 10.1039/B9AY00077A.
- (15) Wang, L.; Cha, X.; Wu, Y.; Xu, J.; Cheng, Z.; Xiang, Q.; Xu, J. Superhydrophobic polymerized n-octadecylsilane surface for BTEX sensing and stable toluene/water selective detection based on QCM sensor. *ACS Omega* **2018**, *3*, 2437-2443, DOI: 10.1021/acsomega.8b00061.
- (16) Adhikari, P.; Alderson, L.; Bender, F.; Ricco, A. J.; Josse, F. Investigation of polymer-plasticizer blends as SH-SAW sensor coatings for detection of benzene in water with high

- sensitivity and long-term stability. *ACS Sens.* **2017**, *2*, 157-164, DOI: 10.1021/acssensors.6b00659.
- (17) Sothivelr, K.; Bender, F.; Josse, F.; Yaz, E. E.; Ricco, A. J. Obtaining chemical selectivity from a single, nonselective sensing film: Two-stage adaptive estimation scheme with multiparameter measurement to quantify mixture components and interferents. *ACS Sens.* **2018**, *3*, 1656-1665, DOI: 10.1021/acssensors.8b00353
- (18) Sothivelr, K.; Bender, F.; Josse, F.; Yaz, E. E.; Ricco, A. J. Quantitative detection of complex mixtures using a single chemical sensor: Analysis of response transients using multi-stage estimation. *ACS Sens.* **2019**, *4*, 1682-1690, DOI: acssensors.9b00564
- (19) Post, M.; Bender, F.; Josse, F.; Ricco, A. J. Application-specific adaptable coatings for sensors: using a single polymer–plasticizer pair to detect aromatic hydrocarbons, mixtures, and interferents in water with single sensors and arrays. *ACS Sens.* **2022**, *7*, 649-657, DOI: 10.1021/acssensors.1c02653.
- (20) Cooper, J. S.; Kiiveri, H.; Chow, E.; Hubble, L. J.; Webster, M. S.; Muller, K.-H.; Raguse, B.; Wieczorek, L. Quantifying mixtures of hydrocarbons dissolved in water with a partially selective sensor array using random forests analysis. *Sens. Actuators B* **2014**, *202*, 279-285, DOI: 10.1016/j.snb.2014.05.094
- (21) Williams, J. H. The molecular electric quadrupole moment and solid-state architecture. *Acc. Chem. Res.* **1993**, *26*, 593-598, DOI: 10.1021/ar00035a005
- (22) Hierlemann, A.; Ricco, A. J.; Bodenhöfer, K.; Göpel, W. Effective Use of Molecular Recognition in Gas Sensing: Results from Acoustic Wave and in Situ FT-IR Measurements *Anal. Chem.* **1999**, *71*, 3022-3035, DOI: 10.1021/ac981311j

- (23) Carey, F. A.; Sundberg, R. J. *Advanced Organic Chemistry 2nd Ed*, Ch. 8, Plenum Press, New York, 1983.
- (24) Takahashi, H.; Suzuoka, D.; Morita, A. Why is Benzene Soluble in Water? Role of OH/ π Interaction in Solvation. *J. Chem. Theory Comput.* **2015**, *11*, 1181-1194, DOI: 10.1021/ct501133u
- (25) Murray, J. S.; Lane, P.; Clark, T.; Riley, K. E.; Politzer, P. s-Hole, p-holes and electrostatically-driven interactions. *J. Mol. Model.* **2012**, *18*, 541-548, DOI: 10.1007/s00894-011-1089-1.
- (26) Mallada, B.; Ondracek, M.; Lamanec, M.; Gallardo, A.; Jimenez-Martin, A.; de la Torre, B.; Hobza, P.; Jelinek, P. Visualization of π -hole in molecules by means of Kelvin probe force microscopy. *Nature Commun.* **2023**, *14*, 4954, DOI: 10.1038/s41467-023-40593-3
- (27) Pluhackova, K.; Jurecka, P.; Hozba, P. Stabilisation energy of C₆H₆···C₆F₆ (X = F, Cl, Br, I, CN) complexes: complete basis set limit calculations at MP2 and CCSD(T) levels. *Phys. Chem. Chem. Phys.* **2007**, *9*, 755, DOI: 10.1039/B615318F.
- (28) Gaussian 09, Revision A.1, Frisch, M. J.; Trucks, G. W.; Schlegel, H. B.; Scuseria, G. E.; Robb, M. A.; Cheeseman, J. R.; Scalmani, G.; Barone, V.; Mennucci, B.; Petersson, G. A.; Nakatsuji, H.; Caricato, M.; Li, X.; Hratchian, H. P.; Izmaylov, A. F.; Bloino, J.; Zheng, G.; Sonnenberg, J. L.; Hada, M.; Ehara, M.; Toyota, K.; Fukuda, R.; Hasegawa, J.; Ishida, M.; Nakajima, T.; Honda, Y.; Kitao, O.; Nakai, H.; Vreven, T.; Montgomery, Jr. J. A.; Peralta, J. E.; Ogliaro, F.; Bearpark, M.; Heyd, J. J.; Brothers, E.; Kudin, K. N.; Staroverov, V. N.; Kobayashi, R.; Normand, J.; Raghavachari, K.; Rendell, A.; Burant, J. C.; Iyengar, S. S.; Tomasi, J.; Cossi, M.; Rega, N.; Millam, J. M.; Klene, M.; Knox, J. E.; Cross, J. B.; Bakken, V.; Adamo, C.; Jaramillo, J.; Gomperts, R.; Stratmann, R. E.; Yazyev, O.; Austin, A. J.;

Cammi, R.; Pomelli, C.; Ochterski, J. W.; Martin, R. L.; Morokuma, K.; Zakrzewski, V. G.; Voth, G. A.; Salvador, P.; Dannenberg, J. J.; Dapprich, S.; Daniels, A. D.; Farkas, O.; Foresman, J. B.; Ortiz, J. V.; Cioslowski, J.; Fox, D. J. Gaussian, Inc., Wallingford CT, **2009**.

- (29) Eberhardt, M., Mruk, R., Znetel & R., Théato, P. Synthesis of pentafluorophenyl(meth)acrylate polymers: New precursor polymers for the synthesis of multifunctional materials. *Euro. Pol. J.* **2005**, *41*, 1569-1575, DOI: 10.1016/j.eurpolymj.2005.01.025.
- (30) Odian, G. *Principles of Polymerization*, Wiley Intersciences, Hoboken, 2004.
- (31) Smirnova, O.; Glazkov, A; Yarsoh, A.; Shkharov, A. Fluorinated Polyurethanes, Synthesis and Properties. *Molecules* **2016**, *21*, 904, DOI: 10.3390/molecules21070904
- (32) Friedt, J.-M.; Rabus, D.; Arapan, L.; Luzet, V.; Chérioux, F.; Nief, N.; Dehez, S.; Ordonez-Varela, J.-R. Package-Less Liquid Phase Sensing Using Surface Acoustic Waves on Lithium Tantalate Oxide. *IEEE Trans. UFFC* **2024**, *71*, 496-505, DOI: 10.1109/TUFFC.2024.3366559
- (33) Fayolle-Guinchard, F., Durand, J., Cheucle, M., Rosell, M., Michelland, R. J., Tracol, J.-P., Le Roux, F., Grundman, G., Atteia, O., Richnow, H. H., Dumestre, A. & Benoit, Y. *J. Haz. Mat.* **2012**, *201-202*, 236-243, DOI: 10.1016/j.jhazmat.2011.11.074.

TABLE OF CONTENTS ARTWORK

